

Effect of Dry-wet Cycle on the Formation of Loess Slope Spalling Hazards

Yuyu Zhang^{a, b*}, Wanjun Ye^a

^a School of Architecture and Civil Engineering, Xi'an University of Science and Technology, Xi'an, Shaanxi, 710054, China.

^b Shaanxi Provincial Communication Construction Group, Xi'an, Shaanxi, 710054, China.

Received 12 March 2018; Accepted 28 April 2018

Abstract


This paper investigates the effect of dry-wet cycle process on the formation of loess slope spalling hazards. Based on the CT scan tests and macroscopic fissures analysis, the fissure variation law of loess samples under different dry-wet cycle times were determined. Through the laboratory direct shear tests, the variation law of shear strength, cohesion and angle of internal friction of loess samples under different dry-wet cycle times and different dry-wet cycle water content variation ranges were discussed. The results show that the natural water contents of Luo-chuan loess were higher than Tong-chuan loess due to its higher contents of clay particles. With the increase of dry-wet cycle times, the internal fissure numbers of loess samples increased dramatically. The value of shear strength and cohesion of loess samples in two different areas decreased dramatically due to the increase of dry-wet cycle times. Higher water content variation ranges of dry-wet cycles led to lower shear strength of loess samples under the same dry-wet cycle times. Loess slope spalling hazards often happened due to the decrease of shear strength and the occurrence of internal fissures in loess induced by the dry-wet cycle process.

Keywords: Loess Slope; Slope Spalling Hazards; Dry-wet Cycle; CT Scan; Direct Shear Test.

1. Introduction

Loess is one of the wind deposited soils which is widely distributed in the Chinese Loess Plateau covering about 6.3×10^5 km², including Gansu, Ningxia, Shaanxi and Henan provinces, etc [1]. Many loess slope spalling hazards happened at Loess Plateau area of China due to the influence of heavy rainfall in the past twenty years (Figure 1) [2-4]. According to the previous research, loess slope spalling hazards can be triggered when water enters into loess slope at a shallow depth, while the saturated zone simultaneously rises from depth [5-8]. The matric suction in unsaturated loess decreased due to the increase of water contents, which induces the decrease of loess shear strength [9-11].

* Corresponding author: yu.yu.zhang@hotmail.com

 <http://dx.doi.org/10.28991/cej-0309133>

➤ This is an open access article under the CC-BY license (<https://creativecommons.org/licenses/by/4.0/>).

© Authors retain all copyrights.

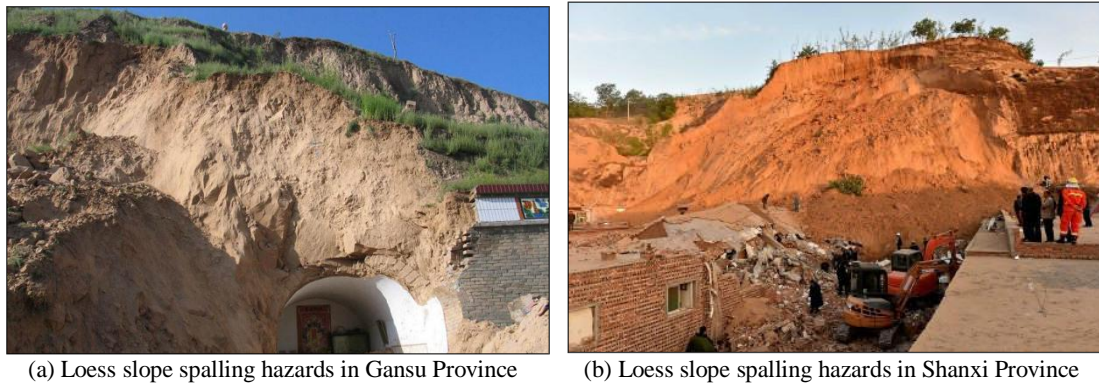


Figure 1. Loess slope spalling hazards in loess area of China

However, in Loess Plateau area of China, for the special climatic conditions of this area, many loess slope spalling hazards often induced by the process of dry-wet cycle [12-15]. According to the previous research, the process of dry-wet cycle can significantly alter the soil moisture distribution and hydro-mechanical behavior, and therefore affect soil performances in various geotechnical applications. Dry-wet cycle can also determine the structure, strength and stability of soil aggregates, which plays an important role in soil physical properties. Besides, desiccation cracks would also develop in soils once it subjected to the dry-wet cycle process. The presence of cracks can significantly increase soil compressibility and hydraulic conductivity [19, 26, 27]. For the natural loess slopes, water enters into loess slopes when it rains and evaporates from loess slopes due to the effects of sunshine. After many times influence of dry-wet cycles, it will lead to the development of internal fissures of loess. Once water enters into the loess fissures, it will continue lead to the development of loess internal fissures and the decrease of loess shear strength. Finally, loess spalling hazards happened due to the influence of this dry-wet process [16-18].

In the past few years, the influence of dry-wet cycle on the soil physical and mechanical properties has received great attention in the geotechnical engineering. Pires (2008) revealed that dry-wet cycle process can cause rearrangement of soil particles, change in the pore system and also induce soil aggregation [19]. Tripathy (2009) found that substantial irreversible accumulation of swelling or shrinkage, as well as significant changes in soil fabric may occur upon dry-wet cycles [20]. Goh (2010) demonstrated that the shear strength characteristics of soils under dry-wet cycle were different [21]. Tang (2011) found that the measured cracking water content and surface crack ratio of the specimen increased in the first three dry-wet cycle times and then tended to reach equilibrium during the subsequent cycle times. The presence of cracks can significantly weaken the soil mechanical performance [22]. Chen and Ng (2013) concluded that the hydro-mechanical behavior of soil was significantly influenced by dry-wet cycle process [23]. Zha (2013) showed that, with the increase of dry-wet cycles, the unconfined compressive strength of soil increased first and then declined [24]. Moayed (2013) investigated the effect of dry-wet cycles on the bearing capacity of lime-silica fume treated soil. They found that the value of CBR (California Bearing Ratio) increased after the first dry-wet cycles, while it started to decrease during the subsequent cycles [25]. Goh (2014) performed a series of tests to understand the shear strength characteristics of unsaturated soils under multiple cycles of drying and wetting. They concluded that the differences between the shear strengths on the drying and wetting paths of the first cycle were found to be more significant than the differences between the shear strengths on the drying and wetting paths of the subsequent cycles [26]. Tang (2016) revealed that the effect of dry-wet cycles on soil profile mechanical behavior depends on soil initial state. The profile structure defects were created after the specimens were subjected to the third times of dry-wet cycle [27].

These studies provided a large number of valuable data for understanding the deformation and mechanical behaviors of soils under the influence of dry-wet cycles. However, most of these studies focused on the investigation of soil strength influenced by the dry-wet cycle process. There are little studies about the variation of internal fissures and mechanical behaviors of loess induced by the process of dry-wet cycle. In order to investigate the mechanical mechanism of loess slope spalling hazards, it is necessary to research both the internal structure variation and the mechanical behaviors of loess when it subjected to the influence of dry-wet cycles. The main purpose of this paper is to investigate the variation law of internal fissures and strength of loess influenced by the dry-wet cycle process. The research results of this paper would provide useful information for the formation mechanism of loess slope spalling hazards induced by dry-wet cycle process in loess area.

2. Research Methodology

Loess samples collected from Luo-chuan loess area and Tong-chuan loess areas were used to study the influence of dry-wet cycle process on the formation mechanism of loess slope spalling hazards.

First, loess samples with different water contents of 12, 15, 20 and 25% were dehumidified to simulate the influence of dry-wet cycle process. There were totally 6 times of dry-wet cycles for each sample in this procedure. Second, loess

samples under different dry-wet cycle times were used to perform the CT scan tests. The variation law of loess internal fissures under different dry-wet cycle times were determined by using CT scan images. Third, loess samples under different dry-wet cycle times and different dry-wet cycle water content variation ranges were used to perform the direct shear strength tests. The variation law of shear strength, cohesion and angel of internal friction of loess samples under different dry-wet cycle times and dry-wet cycle water contents variation ranges were determined by analyzing the results of direct shear strength tests.

3. Materials and Methods

3.1. Properties of test loess

The test loess samples were collected from Luo-chuan area and Tong-chuan area which located at northwest of shaanxi province (Figure 2). Each area was chose to collect 20 groups of loess samples and each group has 6 loess samples. Table 1 shows the physical properties of loess samples from this two areas. Figure 3 shows the slope spalling hazards in this two research areas.



Figure 2. Location of the two research areas



(a) Loess spalling hazards in Luo-chuan area

(b) Loess spalling hazards in Tong-chuan area

Figure 3. Loess slopes of different loess areas

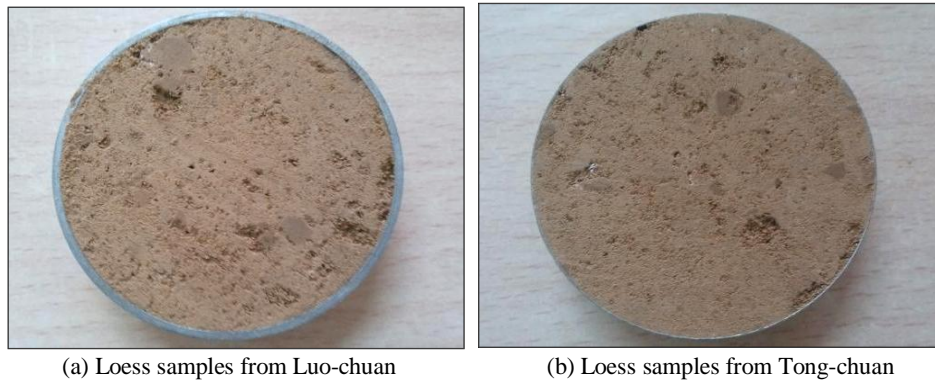
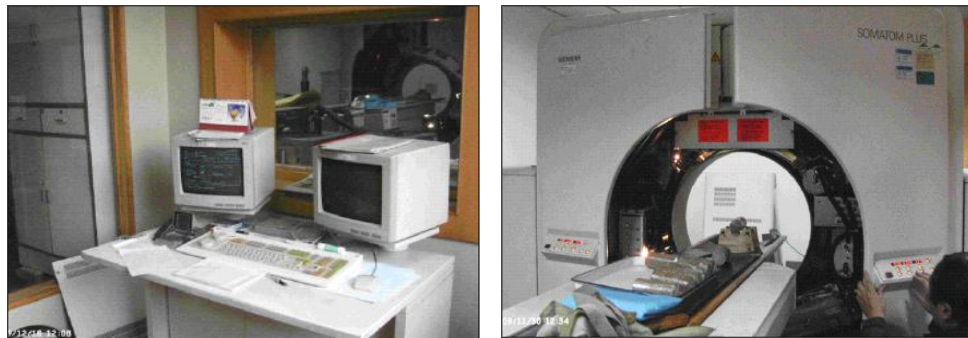
Table 1. Physical properties of loess samples

Area	Natural density (g.cm ⁻³)	Water content (%)	Relative volume mass	Particle size <0.05 mm (%)	Particle size <0.025 mm (%)	Particle size <0.01 mm (%)	Particle size <0.005 mm (%)	Particle size <0.001 mm (%)
Luo-chuan	1.75	15.9	2.69	85.5	57.5	28.5	19.5	1.5
Tong-chuan	1.66	11.7	2.71	87.4	61.0	26.9	5.4	0.5

3.2. Laboratory Tests

3.2.1. CT Scan Tests

This process was used to analyze the internal fissures variation law of loess samples under different dry-wet cycle times. First, the medical injectors (5 ml) were used to add water into the loess samples to obtain the target water contents. Loess samples with different target water contents of 12, 15, 20 and 25% were obtained during this process. Then, loess samples with different target water contents were preserved at a moist container for at least 48 hours for water homogenization. Finally, samples were put in a baking container for 24 hours to remove water. After this dehumidification process, loess samples were placed at the CT scan apparatus to perform the CT scan tests. There were totally 6 times of dry-wet cycles in this procedure. Figure 4 shows loess samples from this two different areas. Figure 5 shows the CT scan apparatus.

**Figure 4. Loess slopes of different loess areas****Figure 5. CT scan apparatus**

3.2.2. Direct Shear Strength Tests

The direct shear strength tests were divided into two procedures. The first procedure was the direct shear strength tests of loess samples under different dry-wet cycle times. First, loess samples with different target water contents (12, 15, 20 and 25%) were put in a baking container for 24 hours to remove water. After each dehumidification process, loess samples with different water contents were taken to perform the direct shear strength tests. There were totally 6 times dry-wet cycles in this procedure. Loess samples were used to perform the shear strength tests under the different vertical pressure of 50, 100, 150 and 200 kPa, respectively. Figure 6 shows the ZJY-3 type of direct shear apparatus.



Figure 6. Direct shear strength apparatus

The second procedure was the direct shear strength tests of loess samples under different dry-wet cycle water content variation ranges. There were four types of dry-wet cycle water content variation ranges of loess samples (5-25, 8-23, 10-20 and 12-17%) in this procedure. Direct shear tests were performed after each dry-wet cycle process. There were totally 6 times of dry-wet cycle process in this procedure.

4. Results and Discussions

4.1. Clay Particle Contents of Loess Samples

As it is shown in Table 1, average mass accumulation of clay particle contents of Luo-chuan loess area was 19.5% while the average mass accumulation of clay particle contents of Tong-chuan loess area was 5.4%. It is noted that the clay particle contents of Luo-chuan loess area was much more than Tong-chuan loess area. The natural water contents of Luo-chuan loess was also higher than Tong-chuan loess. According to the previous research, loess clay particles often composed by montmorillonite, illite and kaolinite which have higher water absorption ability. Therefore, Luo-chuan loess has a higher natural water contents due to its higher clay particle contents.

4.2. Fissure Variation of Loess Samples

Figure 7 shows the fissure variation pictures of loess samples of this two areas under different dry-wet cycle times.

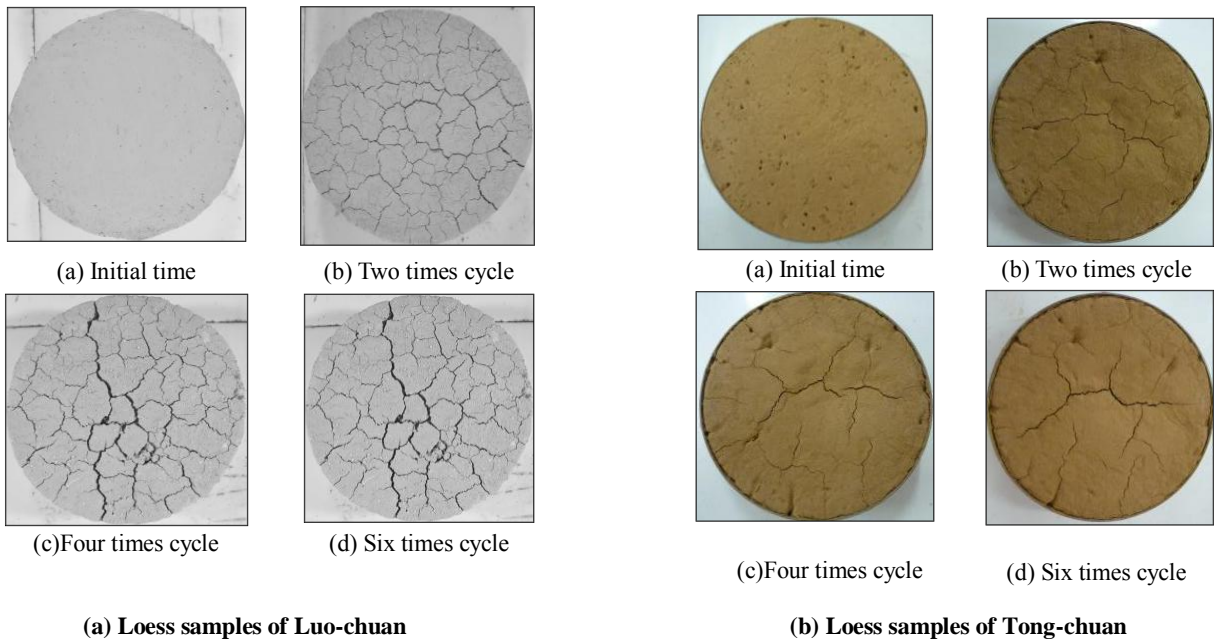


Figure 7. Fissure variation pictures of different loess samples

As it can be seen, there were no fissures in loess samples of this two areas at the initial time of dry-wet cycle. However, after two times of dry-wet cycle process, fissures were appeared at loess samples of both areas. It is noted that loess samples of Luo-chuan had more fissures than loess samples of Tong-chuan. After four times of dry-wet cycle process, fissure numbers of Luo-chuan area increased dramatically, while fissure numbers of Tong-chuan area increased

slowly. After six times of dry-wet cycles, the increase of fissure numbers in loess samples of this two different areas were became stable. It is clearly that fissures occurred in loess samples due to the influence of dry-wet cycle process. With the increase of dry-wet cycle times, fissure numbers increased in loess samples. It is also noted that, fissure numbers in Luo-chuan samples were much more than Tong-chuan samples under the same times of dry-wet cycle process influence. With the increase of dry-wet cycle times, the fissure numbers of Tong-chuan loess samples increased slowly, while the internal fissure numbers of Luo-chuan area increased rapidly. According to the previous study, the increase of fissure numbers of loess induced by the dry-wet cycle process often contributes to the formation of loess spalling hazards.

Due to the complication and irregularity of loess fissures variation, it is difficult to determine the variation law of loess fissures under different times of dry-wet cycle processes. Therefore, fractal theory is often used to analyze the complication and irregularity of rock and soil. Fractal dimension model in the fractal theory can be used to measure the fissure variation process of loess samples. Regarding fissure spacing L and fissure numbers $N(L)$ as horizontal axis and vertical axis, linear relationship between L and $N(L)$ is obtained by:

$$N(L) \propto \left(\frac{1}{L}\right)^D \quad (1)$$

Taking logarithm,

$$D = \lg[N(L)] / \lg(1/L) \quad (2)$$

Here D is fractal dimension; $N(L)$ is fissure numbers; L is fissure spacing.

Figure 8 presents the relation curves between loess sample fissure dimension and dry-wet cycle times.

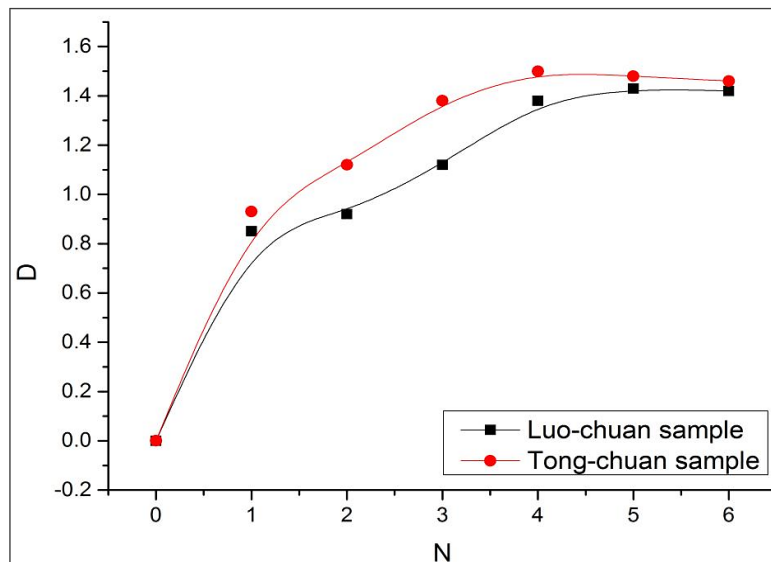
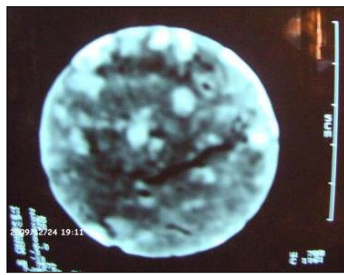


Figure 8. Relation curves between loess sample fissure dimension and dry-wet cycle times

As it is shown in Figure 8, the fractal dimension D can be fitted by using the least square method. According to the relation curve of fractal dimension D influenced by the dry-wet cycle times, the maximum D of Luo-chuan loess samples was 1.5 and it became stable after 5 times dry-wet cycle. The maximum D of Tong-chuan loess samples was 1.2 and it became stable after 4 times cycles. With the increase of D , the fissure spacing decreased and the fissure numbers increased. This theory was precisely reflected the fissure variation in loess samples under the influence of dry-wet cycle process.

4.3. CT Scan Images of Loess Samples

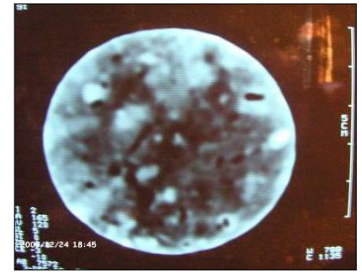
Figure 9 shows the CT scan images of loess samples in Luo-chuan area after the different times of dry-wet cycle process. Figure 10 shows the CT scan images of loess samples in Tong-chuan area after the different times of dry-wet cycle process.



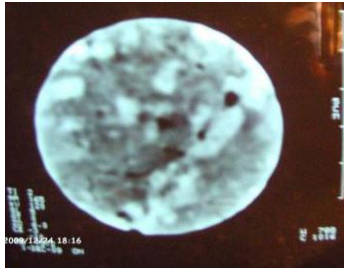
(a) Two times of dry-wet cycle



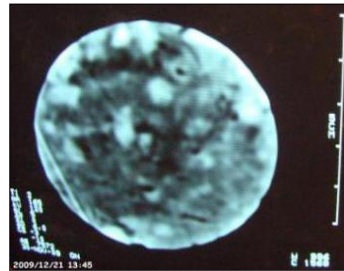
(b) Four times of dry-wet cycle



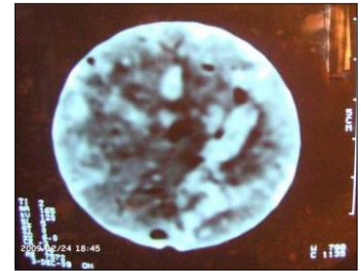
(c) Six times of dry-wet cycle

Figure 9. CT scan images of loess samples of Luo-chuan

(a) Two times of dry-wet cycle



(b) Four times of dry-wet cycle



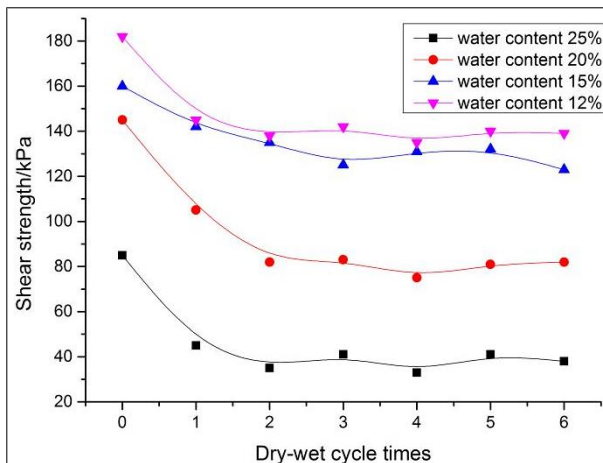
(c) Six times of dry-wet cycle

Figure 10. CT scan images of loess samples of Tong-chuan

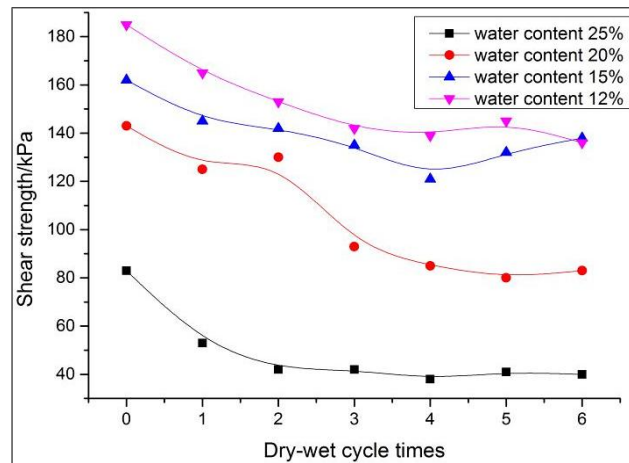
As it is shown in Figure 9 and 10, the internal fissure numbers of Luo-chuan loess samples were much more than Tong-chuan loess samples after two times of dry-wet cycle process. After four times of dry-wet cycle process, the internal fissure numbers increased dramatically in loess samples of both areas. After six times of dry-wet cycle, the internal fissure numbers of Tong-chuan loess samples increased slowly, while the internal fissure numbers of Luo-chuan area still increased rapidly. It is important to note that the internal fissures occurred in loess samples due to the influence of dry-wet cycle process. With the increase of dry-wet cycle times, the internal fissure numbers of loess samples in both areas increased dramatically.

4.4. Effect of Dry-Wet Cycle Times

Figure 11 shows the variation curves between shear strength and dry-wet cycle times of loess samples with different water contents.



(a) Luo-chuan loess samples



(b) Tong-chuan loess samples

Figure 11. Relation curves between shear strength and dry-wet cycle times of loess samples

As it is shown in Figure 11, for Luo-chuan loess samples with different water contents of 25, 20, 15 and 12%, the corresponding initial shear strength were 85, 145, 160 and 182 kPa, respectively. It is noted that the shear strength value of loess samples with higher water contents were smaller than loess samples with lower water contents under the influence of same dry-wet cycle times. After two times of dry-wet cycle process, the shear strength of Luo-chuan loess samples were 38, 78, 137 and 142 kPa, respectively. It is clearly shown that the shear strength of loess samples decreased dramatically at the first three times of dry-wet cycle influence. After three times of dry-wet cycle, the shear strength of

Luo-chuan loess samples became stable.

For loess samples of Tong-chuan area, the initial shear strength of loess samples with water contents of 25, 20, 15 and 12% were 82, 141, 160 and 185 kPa, respectively. After three times of dry-wet cycle, the corresponding shear strength of loess samples were 41, 96, 138, 145 kPa, respectively. The shear strength of loess samples in Tong-chuan area also decreased dramatically after three times of dry-wet cycle process. It is fairly to say that the first three times of dry-wet cycle process had the most important influence on the decrease of shear strength of loess samples. Loess slope spalling hazards often happens due to the decrease of shear strength of loess induced by the dry-wet cycle process.

Figure 12 shows the relation curves between cohesion and dry-wet cycle times of loess sample with different water contents.

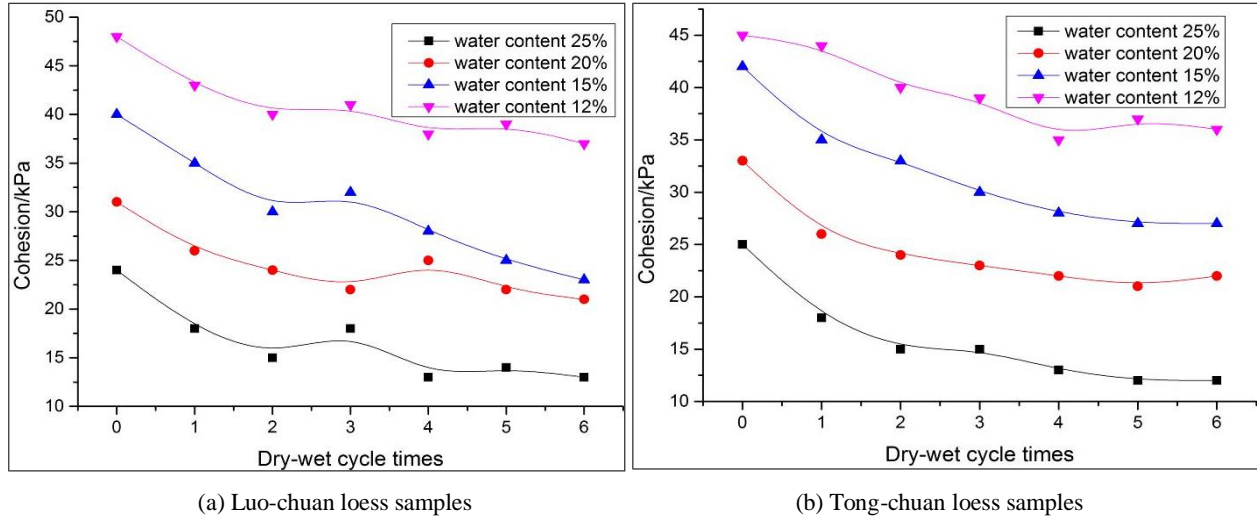


Figure 12. Relation curves between cohesion and dry-wet cycle times of loess samples

As it can be seen in Figure 12, for Luo-chuan loess samples with different water contents of 25, 20, 15 and 12%, the corresponding initial cohesion were 24, 31, 40 and 48 kPa, respectively. With the increase of dry-wet cycle times, the cohesion of loess samples decreased slowly. After five times of dry-wet cycle, the corresponding cohesion were 13, 21, 23 and 37 kPa, respectively. It is noted that the cohesion of loess samples decreased with the increase of dry-wet cycle times. After five times of dry-wet cycle, the cohesion of loess samples became stable. Similarly, loess sample of Tong-chuan area presented the same variation law of cohesion.

Figure 13 shows the relation curves between angle of internal friction and dry-wet cycle times of loess samples with different water contents.

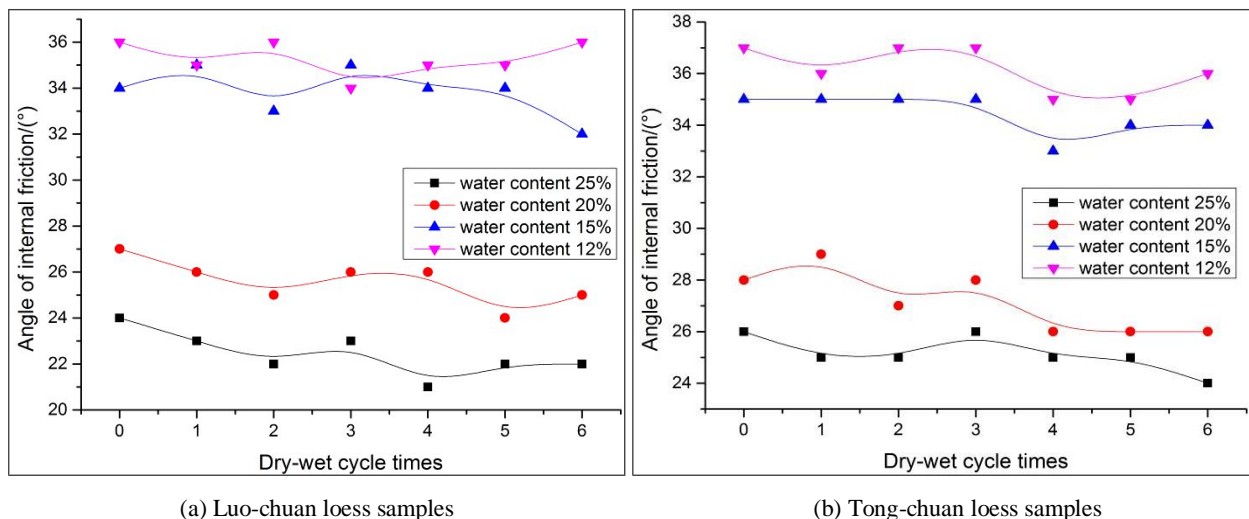


Figure 13. Relation curves between angle of internal friction and dry-wet cycle times

As it can be seen from Figure 13, the value of the angle of internal friction of loess samples stayed stable after each times of dry-wet cycles. For Luo-chuan loess samples with different water contents of 25, 20, 15 and 12%, the initial angle of internal friction were 24° , 27° , 34° and 36° . After six times of dry-wet cycles, the corresponding angle of internal friction were 22° , 25° , 32° , 36° . For Tong-chuan loess samples with water contents of 25, 20, 15 and 12%, the initial angle of internal friction were 26° , 28° , 35° , 37° . After six times of dry-wet cycles, the corresponding initial angle

of internal friction were 24° , 26° , 34° , 36° . It is important to note that the dry-wet cycle process had small effects on the angle of internal friction of loess samples in this two areas.

4.5. Effect of Dry-Wet Cycle Water Content Variation Ranges

Figure 14 shows the relation curves between shear strength and dry-wet cycle times of loess samples with different dry-wet cycle water contents variation ranges. The four types of dry-wet cycle water variation ranges were 5-25, 10-20, 8-23 and 12-17%, respectively.

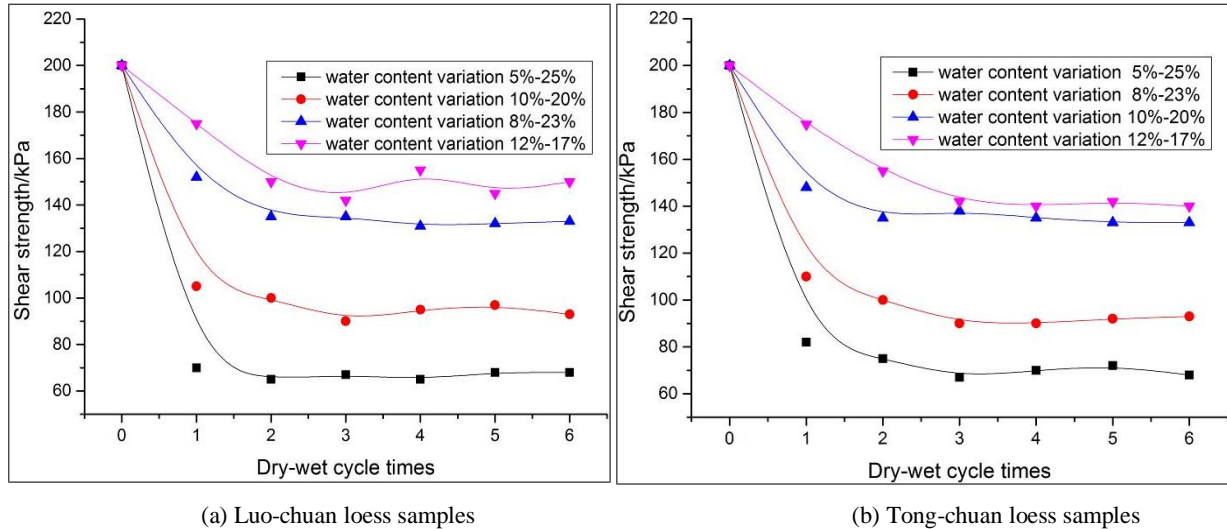


Figure 14. Relation curves between shear strength and dry-wet cycle times

As it is shown in Figure 14, the initial shear strength of Luo-chuan loess samples were 200 kPa. With the increase of dry-wet cycle times, the shear strength of loess samples with different water variation ranges decreased dramatically. After two times of dry-wet cycle process, the shear strength of loess samples with different water variation ranges of 5-25, 10-20, 8-23 and 12-17%, were 68, 93, 133 and 155 kPa, respectively. It is clearly shown that loess samples with higher water contents variation ranges presented lower shear strength value. With the increase of dry-wet cycle times, the shear strength of loess samples with higher water contents variation ranges decreased more dramatically than loess with lower water contents variation ranges. Loess from Tong-chuan presented the same variation law of shear strength under different dry-wet cycle water contents variation ranges.

5. Conclusion

- The clay particle contents of Luo-chuan loess area were more than those in Tong-chuan loess area. The natural water contents of Luo-chuan loess were higher than Tong-chuan loess due to it's higher contents of clay particles.
- Loess samples of Luo-chuan presented more fissure numbers than loess samples of Tong-chuan under the same dry-wet cycle times. With the increase of dry-wet cycle times, the fissure numbers of Tong-chuan loess samples increased slowly, while the internal fissure numbers of Luo-chuan area increased rapidly.
- The maximum D value of Luo-chuan loess samples was 1.5 and it became stable after 3 times dry-wet cycles. The maximum D value of Tong-chuan loess samples was 1.2 and it became stable after 5 times cycles. With the increase of fractal dimension D, the fissure spacing of different loess samples decreased and the fissure numbers increased.
- The internal fissures occurred in loess samples due to the influence of dry-wet process. The internal fissure numbers of Luo-chuan loess samples were much more than Tong-chuan loess samples after the same times of dry-wet cycle process. With the increase of dry-wet cycle times, the internal fissure numbers in loess samples of both areas increased dramatically.
- The shear strength and cohesion of loess samples from different two areas decreased dramatically due to the increase of dry-wet cycle times. The first two or three times of dry-wet cycle had the most significant influence on the decrease of loess shear strength and cohesion.
- Higher water content variation ranges of dry-wet cycles led to lower shear strength of loess samples under the same dry-wet cycle times. Loess slope spalling hazards often happened due to the development of loess fissures and the decrease of shear strength of loess induced by the dry-wet cycle process.

6. Acknowledgements

The author would like to thank Professor Wanjun Ye for his guidance and support.

7. Funding

This work was funded by National Natural Science Foundation of China (Grant No.41672305; N0.41172262). Key Scientific and Technological innovation team of Shaanxi province (No. 2014KTC-30)

8. References

- [1] L.Z. Wu, Y. Zhou, P. Sun, J.S. Shi, G.G. Liu, L.Y. Bai. "Laboratory characterization of rainfall-induced loess slope failure". *Catena*. 150 (November 2016): 1-8. DOI: <http://dx.doi.org/10.1016/j.catena.2016.11.002>.
- [2] Derbyshire, E. Meng, X. M., Dijkstra, T.A. "Landslides in the Thick Loess Terrain of North-West China. *Engineering Geology*". 59 (January 2001): 201-202. DOI: 10.1016/S0013-7952(00)00067-3.
- [3] Wang, H.B., Zhou, B., Wu, S.R., Shi, J.S. "Characteristic analysis of large-scale loess landslides: a case study in Baoji City of Loess Plateau of Northwest of China". *Natural Hazards and Earth System Sciences*. 11 (July 2011): 1829-1837. DOI: 10.5194/nhess-11-1829-2011.
- [4] Peng J.B, Fan, Z. J, Wu D., Zhuang J.Q. "Heavy rainfall triggered loess-mudstone landslide and subsequent debris flow in Tianshui, China". *Engineering Geology*. 186 (August 2014): 79-90. DOI: <http://dx.doi.org/10.1016/j.enggeo.2014.08.015>.
- [5] Wang, G.H., Zhang, D.X., Furuya, G., Yang, J. "Pore-pressure generation and fluidization in a loess landslide triggered by the 1920 Haiyuan earthquake, China: a case study". *Engineering Geology*, 174 (March 2014) : 46-45. DOI: <http://dx.doi.org/10.1016/j.enggeo.2014.03.006>.
- [6] Zhang, M.S., Liu, J. "Controlling factors of loess landslides in western China". *Environment Earth Sciences*, 59 (2010): 1671-1680. DOI: 10.1007/s12665-009-0149-7.
- [7] Wang, J.J, Liang, J.Y., Zhang, H.P., Wu, Y. "A loess landslide induced by excavation and rainfall". *Landslides*. 11 (February 2014): 14-152. DOI: 10.1007/s10346-013-0418-0.
- [8] Shi, J.S, Wu L.Z, Wu S.R., Li B., Wang, T., Xin, P. "Analysis of the causes of large-scale loess landslide in Baoji, China". *Geomorphology*. 264 (January 2016): 109-117. DOI: 10.1016/j.geomorph.2016.04.013.
- [9] Anderson S.A., Sitar N. "Analysis of rainfall-induced debris flows". *Journal of Geotechnical Engineering*". 121 (July 1995): 544-552. DOI: 10.1061/(ASCE)0733-9410(1995)121:7(544).
- [10] Sorbino G., Nicotera, M.V. "Unsaturated soil mechanics in rainfall-induced flow landslides". *Engineering Geology*. 165 (October 2013):105-132. DOI: 10.1016/j.enggeo.2012.10.008.
- [11] Xu L, Qiao X.J, Wu C.X, Dai F.C. "Cause of landslide recurrence in a loess platform with respect to hydrological processes". *Natural Hazards*. 64 (2012): 1657-1670. DOI: 10.1007/s11069-012-0326-y.
- [12] Pranshoo Solanki, Musharraf Zaman. "Effect of wet-dry cycling on the mechanical properties of stabilize subgrade soils". 6 (February 2014): 250-256. *Geotechnical Special Publication*. Doi: 10.1061/9780784413272.351.
- [13] Xing rong Liu, Zi juan Wang. "Macro/Microtesting and Damage and Degradation of Sandstones under Dry-Wet Cycles". *Advances in Materials*. 1 (Janaury 2016): 1-16. DOI: 10.1155/2016/7013032.
- [14] Jie Xiao, He-ping Yang, Jun-hui Zhang, Xian-yuan Tang. "Surficial Failure of Expansive Soil Cutting Slope and Its Flexible Support Treatment Technology". *Applied Mechanics and Materials*. 35 (2018): 30-42. DOI: <https://doi.org/10.1155/2018/1609608>.
- [15] Ai Bing Jin, Fu Geng Deng. "Research on Stability Mechanism of Fissured Loess Slope Influenced by Rainfall and Evaporation". 170 (May 2012): 380-385. DOI: 10.4028/www.scientific.net/AMM.170-173.380.
- [16] H. Rahardjo, E. C. Leong. "Effect of antecedent rainfall on pore-water pressure distribution characteristics in residual soil slopes under tropical rainfall". *Hydrological Processes*. 22 (February 2018): 506-523. DOI: 10.1002/hyp.6880.
- [17] S.E. Cho, S.R. Lee. "Instability of unsaturated soil slopes due to infiltration". *Computers and Geotechnics*. 28 (April 2001): 185-208. DOI: 10.1016/S0266-352X(00)00027-6.
- [18] Ren-ming Ma, Chongfa Cai. "Evaluation of soil aggregate microstructure and stability under wetting and drying cycles in two Ultisols using synchrotron-based X-ray micro-computed tomography". *Soil and Tillage Research*. 149 (June 2015): 120-125. DOI: 10.1016/j.still.2014.12.016.
- [19] Pires, L.F., Cooper. Micromorphological analysis to characterize structure modifications of soil samples submitted to wetting and drying cycles. *Catena*. 72 (January 2008): 297-304. DOI: 10.1016/j.catena.2007.06.003/.
- [20] Tripathy, S., Kanakapura, S., Rao, S. Cyclic swell-shrink behavior of a compacted expansive soil. *Geotechnical and Geological Engineering*. 27 (February 2009): 89-103. DOI: 10.1007/s10706-008-9214-3.
- [21] Goh, S.G., Rahardjo, H., Leong, E.C. Shear strength equations for unsaturated soil under drying and wetting. *Journal of Geotechnical and Geoenvironmental Engineering*. 136 (April 2010): 594-606. DOI: 10.1061/(ASCE)GT.1943-5606.0000261.
- [22] Tang, C.S., Cui, Y.J., Shi, B., Tang, A.M., Liu, C. Desiccation and cracking behavior of clay layer from slurry state under

wetting-drying cycles. *Geoderma*. 166 (October 2011): 111-118. DOI: 10.1016/j.geoderma.2011.07.018.

[23] Chen, R., Ng, C.W.W. Impact of wetting-drying cycle on hydro-mechanical behavior of an unsaturated compacted clay. *Applied Clay Science*. 86 (December 2013): 38-46. DOI: 10.1016/j.clay.2013.09.018.

[24] Zha, F.S., Liu, J.J., Xu, L., Cui, K.R. *Journal of Central South University*. Effect of cyclic drying and wetting on engineering properties of heavy metal contaminated soils solidified/stabilized with fly ash. 20 (July 2013): 1947-1952.

[25] Moayed, R.Z., Lahiji, B.P., Daghigh, Y. Effect of wetting-drying cycles on CBR values of Silty subgrade soil of karaj railway. *Proceedings of the 18th International Conference on Soil Mechanics and Geotechnical Engineering*. 18 (September 2013): 1321-1324.

[26] Goh, H.R, E.C. Shear strength of unsaturated soils under multiple drying-wetting cycles. *Journal of Geotechnical and Geoenvironmental Engineering*. 140 (February 2014):90-108. DOI: 10.1061/(ASCE)GT.1943-5606.0001032.

[27] Tang C.S., Wang D.Y., Shi B. Effect of wetting-drying cycles on profile mechanical behavior of soils with different initial conditions. *Catena*. 139(April 2016): 105-116. DOI: 10.1016/j.catena.2015.12.015.